2024 European Control Conference (ECC)
June 25-28, 2024. Stockholm, Sweden

Identification of a dynamic model of pain and fear characteristics during vaginal dilation exercises

Roxanne R. Jackson, Damiano Varagnolo, Marieke Dewitte, and Steffi Knorn

***Abstract*— Treating dyspareunia, i.e., pain during vaginal penetrative sexual intercourse, may include vaginal dilation exercises that are often perceived as uncomfortable (or worse) by patients. Being able to accurately predict the pain and fear levels of these subjects during the treatments is thus instrumental in designing effective personalized dilation patterns for therapies. Toward this goal, in this paper, we combine an existing qualitative model of vaginal pressure, pain, and fear relations with experimental data obtained during medical trials to derive a parametric model. More precisely, we: *1)* analyze how to deal with the identifiability issues caused by the presence of uninterpretable parameters in the original model, *2)* use this analysis to derive a novel model that is better suited for data-driven learning purposes, *3)* perform a parameter identification using weighted least squares on online and offline measurement data, and *4)* test the capability of the overall approach in predicting signals that are proxies of fear and pain levels, comparing the performance one obtains with this refined approach against purely black box Autoregressive moving average exogenous (ARMAX) models. The results indicate that the proposed method works best as a predictive model of fear and pain levels in response to visual and pressure stimuli but still lacks a high level of generalizability.**

I. Introduction

Genito-pelvic pain/penetration disorders (GPPPDs), for example, painful experiences during sexual intercourse, is estimated to affect a great number of people with vaginas (e.g., 30–40 % are estimated to suffer from prolonged periods of painful sexual intercourse experiences at some point during their lives [1, Chap. 2]). GPPPDs may be caused by physiological, psychological, and social factors, and the union of these [1, Chap. 3]. Further, interpersonal and related factors such as a hostile partner and other psycho-social impacts contribute to the maintenance, exacerbation, and chronicization of GPPPDs. Affected people are more likely to develop co-morbid sexual difficulties, negative affect, and relationship concerns [1, Chap. 3], which all significantly diminish their quality of life.

Treatments for GPPPDs include psychological treatments, e.g., cognitive behavioral therapies, and physiological treatments such as the use of Vaginal Trainers (VTs) [2]. VTs, or dilators, are tube-shaped devices used to stretch the vaginal duct. They often range from small (the size of a finger) to large. VTs are a widely recommended treatment for GPPPDs and are a required part of the postoperative care regimen following vaginoplasty surgery [2], [3].

VTs as a treatment method are invasive and lengthy, and many patients experience intense pain and failure when trying to insert even the smallest dilator [4]. Treatment drop-out rates force women to live with their debilitating disorders. Thus, there is an obvious societal need to adapt physiological treatments for GPPPDs to increase their appeal and consider the psychological impact of invasive treatment methods.

A. Literature review

When it comes to existing models in literature for the dynamics of genital pain during penetrative intercourse, it is known that fear induces the activity of the pelvic floor muscles, [5], [6]. Further, if the pelvic floor muscles are active when attempting vaginal penetration, both lubrication and vasocongestion levels decrease since the increased pressure on the vulvar and vaginal skin leads to reduced blood flow and lubrication [7], [8]. Importantly, this relationship depends on the timing: initial stages of arousal lead to an initial relaxation of the pelvic floor. As arousal increases, the deeper-located pelvic floor muscles contract to achieve the orgasmic phase, but these contractions do not affect the lubrication and vasocongestion [6]. The previous implications then suggest that low physiological arousal or active pelvic floor muscles lead to genital pain when penetration is attempted. This logical chain is consistent with other existing medical literature on the subject, e.g., [9]–[11].

To our knowledge, the relations mentioned above have not been interconnected using explainable ordinary differential equations. Indeed, all the models in the aforementioned medical literature focus on understanding implications and cause-effect relationships; in this specific field of medicine, though, there is a lack of mathematical models that can be used to build forecasters of when a specific person will start for example developing unbearable pain if subjected to stimuli. Towards closing this gap, [12] proposed a model to describe the dynamics of pleasure and arousal response to visual stimuli and vaginal pressure called the Circle Of Pleasure (COP), seen on the left side of Figure 1 and the pressure vs. pain mechanisms referred to as the Circle Of Fear (COF) and shown on the right side of Figure 1. However, even though the model was based on the implications published in the medical literature and expert knowledge, it is yet to be validated with data nor exploited for creating further understandings of how treatments can be improved.

R. R. Jackson and S. Knorn are with the Department of Control Engineering at the Technical University of Berlin, Germany. {jackson | knorn}@tu-berlin.de

D. Varagnolo is with the Department of Engineering Cybernetics at the Norwegian University of Science and Technology, Norway, and the Department of Information Engineering at the University of Padova, Italy. damiano.varagnolo@ntnu.no

M. Dewitte is with the Department of Experimental Health Psychology at Maastricht University, the Netherlands marieke.dewitte@maastrichtuniversity.nl

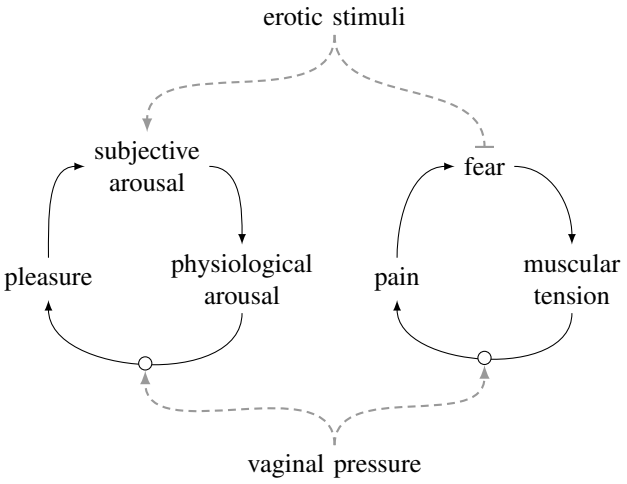

Fig. 1: Schematic representation of the qualitative model from [12]. This model assumes erotic stimuli to inhibit fear by diminishing fearful thoughts. Pressure stimuli are instead assumed to stimulate muscular tension, and thus potentially lead to pain. Depending on the psychophysical status, pressure stimuli are thus supposed to potentially lead to either pain or pleasure.

B. Statement of contributions

From the domain side, we contribute with increasing the scientific understanding of understanding the effects of pain and fear, and provide models that may help designing vaginal dilation therapies with a smaller likelihood of development of undesirable effects in patients. From the methodological side, we:

1) extend upon the qualitative model in [12] to make it suitable for data-driven identification purposes;
2) propose a method for dealing with ill-posed problems with uninterpretable parameters and a combination of both online and offline measurements;
3) analyze the performance of the proposed grey-box model compared to black-box methods with interpolated data; and
4) perform a practical identifiability analysis that both indicates which experiment design factors are important in this specific domain, but that also may serve as a template for similar analyses in other contexts.

C. Organization of the manuscript

Section II presents the medical trial setting and the collected data. Section III extends the model in [12] to make it more suitable for quantitative analysis. Section IV presents methods for dealing with ill-posed problems, identifiability, unknown parameter spaces, and online-offline measurements. Section V presents the results from our quantitative analyses for the COF, followed by Section VI, which concludes the manuscript with some remarks on what methods could be adopted to improve the model further.

II. Medical trial setup and data

Medical trials were executed at Maastricht University Hospital to investigate how the Pelvic Floor Muscles (PFMs) respond to forced vaginal dilation [13]. The data in this trial comprises the responses of healthy people with vaginas to the gradual vaginal dilation induced by an inflatable balloon inserted at the introitus while watching sequences of different 5-minute-long erotic or non-erotic films in a controlled laboratory environment. The medical device is called a Vaginal Pressure Inducer (VPI), shown in Figure 2.

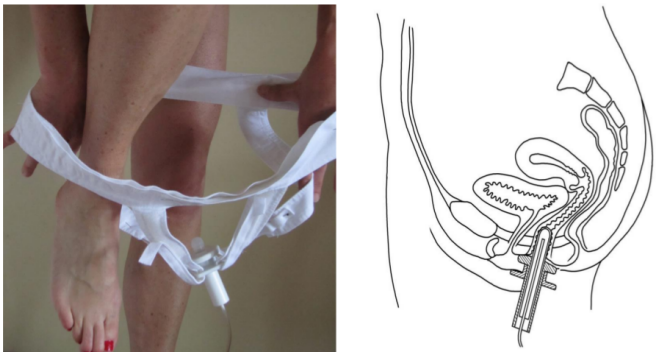

Fig. 2: Picture of the VPI (left) and schematic description of its utilization (right). The balloon is gradually filled with water by a controlled pump. The device measures exerted pressure by sensing the force exerted by the pump.

A. Participants and experimental protocol

Given the limitations about the number of recruitable participants, and aiming to create a homogeneous group in terms of demographics, the study included 42 healthy women aged between 18 and 45 years who had been in a steady heterosexual relationship for at least 3 months, and who in this period had been sexually active including coitus. Each woman participated in individual sessions where they recorded their perceived level of comfort with an opportune slider while wearing the VPI and watching pre-defined film sequences. Importantly, the participants could prematurely end the experiments with a stop button as soon as the pressure level felt unpleasant– forcing an instant deflation of the balloon.

Each session started with an acclimatization phase including the expansion of the VPI followed by showing a high-arousal sexual film without inducing vaginal pressure (control condition). Then, each woman watched four films (a high-arousal & sexual, a low-arousal & sexual, a high-arousal & nonsexual, and neutral) in random order with pressure induced by the VPI and intermittent distraction tasks.

B. Data

During the experiment, the induced pressure in the water was measured at the pump as an indirect measure of the pelvic floor muscle activity at a frequency of 2 Hz. The reported subjective pleasure (on a scale between 0 and 100) was also recorded as well as the times when patients stopped the experiment to force the deflation of the balloon. A typical sample of the corresponding time series is shown in Figure 3.

III. A dynamic model of the Circle Of Fear

The qualitative model presented in [12] as shown in Figure 1 has inputs u_{pressure} and u_{stimulus}, corresponding

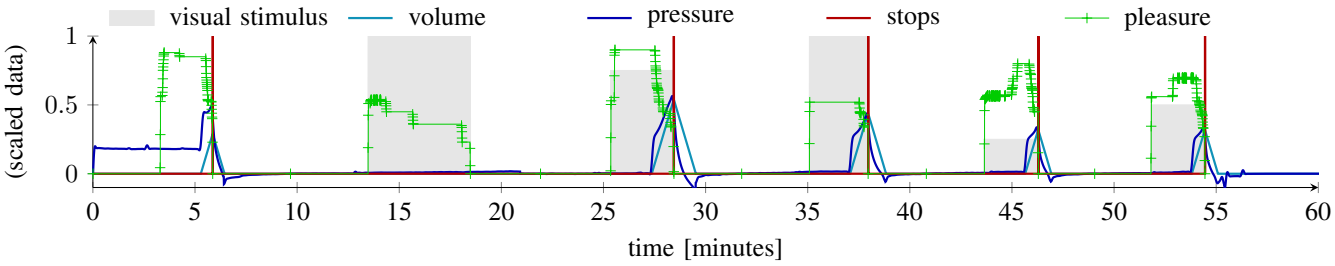

Fig. 3: A typical patient dataset (min-max scaled). The six films; neutral (acclimatization), high arousal and sexual (control condition), low arousal and sexual, high arousal and sexual, low arousal and non-sexual, high arousal and non-sexual; started at minutes 3, 13, 26, 35, 43 and 52, respectively. Inflation of the VPI is shown by the volume plot and the pressure measured in the balloon is indicated by the pressure curve. The pleasure is a subjective measure changed by the patient with a slider and the stops indicate that the patient terminated the experiment early which resulted in an instant deflation of the VPI.

respectively to induced vaginal pressure levels through the VPI, and an erotic stimulus due to watching different types of films during the experiment. These inputs are considered to be non-negative and less than one. We also note the existence of the indirect measurement, the so-called "stop events", i.e., where patients decide to stop the inflation of the VPI and force its deflation, likely due to degrading comfort levels. Further, the model is a positive system.

A. Process model

Referring to Figure 1, the right part of the model describes the feedback loop between fear, muscular tension, and pain by means of

$$\dot{x}_{\text{pain}}(t) = -\theta_1 x_{\text{pain}}(t) + \theta_2 \sqrt{x_{\text{muscles}}(t)}\, u_{\text{pressure}}(t), \quad (1a)$$

$$\dot{x}_{\text{muscles}}(t) = -\theta_3 x_{\text{muscles}}(t) + \theta_4 x_{\text{fear}}(t), \quad (1b)$$

$$\dot{x}_{\text{fear}}(t) = -\theta_5 x_{\text{fear}}(t) - \theta_6 x_{\text{fear}}(t) u_{\text{stimulus}}(t) + \theta_7 x_{\text{pain}}(t)\,. \quad (1c)$$

For $x_{\text{COF}} = \begin{bmatrix} x_{\text{pain}} & x_{\text{muscles}} & x_{\text{pain}} \end{bmatrix}^\top \in \mathbb{R}^3$, we use the shorthand $\dot{x}_{\text{COF}} = f(x_{\text{COF}}, u, \theta)$, where $u = \begin{bmatrix} u_{\text{pressure}} & u_{\text{stimulus}} \end{bmatrix}^\top \in [0,1]$ and $\theta \in \mathbb{R}^{11}$. In (1a), the term $\sqrt{x_{\text{muscles}}} u_{\text{pressure}}$ models the assumption that pelvic muscle activity before or at the beginning of penetration may lead to pain in the patient – if there is some vaginal pressure applied. In this framework, x_{muscles} acts as an *enabling* factor since the influence of u_{pressure} on x_{pain} increases relatively more when x_{muscles} is small rather than large. This is compliant with the findings in [14]. Besides this, equation (1b) qualitatively captures the fact that fear leads to muscular tension. Finally, (1c) models the fact that pain solicits fear. The effects of erotic stimuli are instead modeled with the intuition that positive erotic stimuli may temper fear. Thus, if the patient is being stimulated, i.e., $u_{\text{stimulus}} > 0$, while feeling fear then $x_{\text{fear}} u_{\text{stimulus}}$ acts as a fear-reduction mechanism. Finally, we note the presence in all three equations above of opportune first terms on the right-hand side that make the origin an asymptotically stable point; this captures the intuition that in the absence of external stimuli the person should ideally arrive at a neutral resting condition.

B. Measurement model

We start the model-modification effort by rephrasing the experimental data in Section II-B in terms of the information introduced in Section III-A, i.e., define the measurement model for the COF from the given data. More specifically, we postulate that the measurement data about vaginal pressure and the probability of the "stops" are measurements of opportune transformations of the variable x_{COF} in the following sense:

$$y_{\text{pressure}}(t) = \theta_8 x_{\text{muscles}}(t) + \theta_9 u_{\text{pressure}}(t), \quad (2a)$$

$$y_{\text{stop}}(t) = \theta_{10} x_{\text{fear}}(t) + \theta_{11} x_{\text{pain}}(t)\,. \quad (2b)$$

More precisely, (2a) captures the following considerations: first, the measured pressure is the total pressure at the end of the water pipe connecting the VPI with its pump. The quantities resisting this pressure are then two: the actual pressure stimulus applied to the vaginal duct and the activation of PFMs. The equation captures the fact that there exists a proportional (but typically unknown) relation between the muscular pressure and its effects on y_{pressure}. (2b) instead, models the fact that a patient presses the stop button due to a combination of pain and fear. Additionally, although y_{stop} is physically a binary variable, we anyway model it as a continuous one, since we wish to use this value as a proxy for the likelihood that a patient will stop the experiment at any time.

We use the notation $y = \begin{bmatrix} y_{\text{pressure}} & y_{\text{stop}} \end{bmatrix}^\top$ where $y = h(x_{\text{COF}}, u, \theta)$. We further denote the measurements by $Y_M = \begin{bmatrix} y_M(t_1)^\top & \dots & y_M(t_N)^\top \end{bmatrix}^\top \in \mathbb{R}^{n_d}$, where n_d is the number of measurements, noting that the y_{pressure} measurements are taken at a constant sampling time, i.e., online, and y_{stop} are only taken when the stop button is pushed; i.e., offline. Furthermore, the measurement model responses are denoted as $Y(u,\theta) = \begin{bmatrix} y(u,\theta,t_1)^\top & \dots & y(u,\theta,t_N)^\top \end{bmatrix}^\top \in \mathbb{R}^{n_d}$.

IV. Methods for identification of the Circle Of Fear model

We show now that, as often happens with biological systems (see [15]–[17]), the available measurements from Section III-B are not rich enough to guarantee the identifiability of the original vaginal pressure model. In this section

we propose a method to deal with such problems where, additionally, we have some sparse measurement data.

A. Detecting practical identifiability

Unstable and inaccurate solutions to parameter estimation problems in nonlinear system identification can be caused by over-parameterization (where some parameters have little to no influence on the observations), a mismatch of the model structure, limited experimental information, and/or inaccurate initial parameter guesses [18].

1) Background on subset selection: Subset selection mitigates the issues of ill-posed problems. Here, we follow the method proposed in [18] and [19] where the ill-conditioning is assessed by means of sensitivity matrices. In our case, this matrix computes the sensitivity of the observations with respect to the model parameters, defined by

$$S(u,\theta) = \frac{\mathrm{d}Y(u,\theta)}{\mathrm{d}\theta}\,, \tag{3}$$

where $S(u,\theta) \in \mathbb{R}^{n_d \times n_p}$ for n_p parameters. We can further define $\tilde{S}(u,\theta) = W^{1/2}S(u,\theta)$ as the scaled sensitivity matrix to account for a weighting factor W in the Parameter Identification (PI) problem; see Section IV-C.

To calculate the sensitivity of the output, we use the chain rule

$$\frac{\mathrm{d}Y(u,\theta)}{\mathrm{d}\theta} = \frac{\partial h(X,u,\theta)}{\partial X}\frac{\mathrm{d}X}{\mathrm{d}\theta} + \frac{\partial h(X,u,\theta)}{\partial \theta}\,. \tag{4}$$

We then define the state sensitivities to be $X_S = \frac{\mathrm{d}X}{\mathrm{d}\theta}$ where

$$\dot{X}_S = \frac{\mathrm{d}X_S}{\mathrm{d}t} = \frac{\mathrm{d}}{\mathrm{d}t}\frac{\mathrm{d}X}{\mathrm{d}\theta} = \frac{\mathrm{d}}{\mathrm{d}\theta}\frac{\mathrm{d}X}{\mathrm{d}t} = \frac{\mathrm{d}}{\mathrm{d}\theta}f(X,u,\theta)$$

and applying the chain rule gives

$$\begin{aligned}\dot{X}_S &= \frac{\partial f(X,u,\theta)}{\partial X}\frac{\mathrm{d}X}{\mathrm{d}\theta} + \frac{\partial f(X,u,\theta)}{\partial \theta} \\ &= \frac{\partial f(X,u,\theta)}{\partial X}X_S + \frac{\partial f(X,u,\theta)}{\partial \theta}\,.\end{aligned} \tag{5}$$

We thus need to compute the Jacobians $\frac{\partial f(X,u,\theta)}{\partial X}$, $\frac{\partial f(X,u,\theta)}{\partial \theta}$ to solve (5) and use the Jacobians $\frac{\partial h(X,u,\theta)}{\partial X}$, $\frac{\partial h(X,u,\theta)}{\partial \theta}$ to calculate the sensitivities in (4).

To analyze the ill-conditioning of $\tilde{S}$, we use Singular Value Decomposition (SVD) such that

$$\tilde{S} = UZV^\top\,. \tag{6}$$

In (6), $U \in \mathbb{R}^{n_d \times n_d}$ and $V \in \mathbb{R}^{n_p \times n_p}$ are orthogonal matrices, and $Z = \mathrm{diag}(\zeta_1, \ldots, \zeta_{n_p})$, where ζ_i are the ordered singular values of $\tilde{S}$, i.e., $\zeta_1 > \zeta_2 > \cdots > \zeta_{n_p}$.

The presence of small singular values in Z indicates that $\tilde{S}$ is ill-conditioned and hence rank deficient [20]. [18] introduce an ε-threshold to put a lower bound on the Singular Values (SVs) determined by the maximum condition number $\kappa_{\max}(\tilde{S})$ and the collinearity index $\gamma_{\max}(\tilde{S})$. The condition number is calculated with $\kappa(\tilde{S}) = \frac{\zeta_1}{\zeta_{n_p}}$ [21]. When $\kappa(\tilde{S}) \approx 1$, the matrix is well-conditioned, where $\kappa(\tilde{S}) = 1$ implies that the columns of $\tilde{S}$ are orthogonal. Conversely, near linear dependence results in a large κ. The degree of linear independence is then determined by the collinearity index $\gamma(\tilde{S}) = \frac{1}{\zeta_{n_p}}$. Large values of $\gamma(\tilde{S})$ indicate linear dependence and poor identifiability. Common empirical bounds, proposed in [22], are $\kappa_{\max}(S) \approx 1000$ and $\gamma_{\max}(S) = 10$. The ε-threshold is then defined as $\varepsilon = \max\left\{\frac{\zeta_1}{\kappa_{\max}(\tilde{S})}, \frac{1}{\gamma_{\max}(\tilde{S})}\right\}$. We can use the ϵ-threshold to determine the largest collection of linearly dependent columns of $\tilde{S}$, i.e., sets the number m such that $\zeta_1 > \zeta_2 > \cdots > \zeta_m > \varepsilon > \zeta_{m+1} > \cdots > \zeta_{n_p}$.

In subset selection, the number of parameters in the identifiable parameter subset corresponds to m. The parameter vector is reordered by a QR decomposition of $\tilde{S}$ where the matrix $P \in \mathbb{R}^{n_p \times n_p}$ reorders $\tilde{S}$ according to linear dependence such that $\tilde{S}P = QR$ for the orthogonal matrix $Q \in \mathbb{R}^{n_d \times n_d}$ and the upper triangular matrix with decreasing diagonal elements $R \in \mathbb{R}^{n_d \times n_p}$. We can then use P to select the identifiable parameters by $\tilde{\theta} = P\theta$.

2) Subset selection for the COF: We can thus analyze the practical identifiability of our system by performing a SVD of the sensitivity $S(u,\theta)$ which results in the Singular Value Spectrum (SVS) shown in Figure 4 with the ε-threshold set to 0.14. Using this ε-threshold results in six identifiable parameters $\tilde{\theta} = \begin{bmatrix}\theta_2 & \theta_5 & \theta_6 & \theta_8 & \theta_9 & \theta_{11}\end{bmatrix}^\top$ and five non identifiable parameters $\phi = \begin{bmatrix}\theta_1 & \theta_3 & \theta_4 & \theta_7 & \theta_{10}\end{bmatrix}^\top$.

We thus choose the fixed values $\phi = \begin{bmatrix}0.1 & 6 & 1 & 1 & 0.75\end{bmatrix}^\top$, where ϕ_2 was chosen from [23], and the other values were chosen from trial-and-error. The new system equations become

$$\begin{aligned}\dot{x}_{\text{pain}}(t) &= -\phi_1 x_{\text{pain}}(t) \\ &\quad + \tilde{\theta}_1\sqrt{x_{\text{muscles}}(t)}u_{\text{pressure}}(t), &\text{(7a)}\\ \dot{x}_{\text{muscles}}(t) &= -\phi_2 x_{\text{muscles}}(t) + \phi_3 x_{\text{fear}}(t), &\text{(7b)}\\ \dot{x}_{\text{fear}}(t) &= -\tilde{\theta}_2 x_{\text{fear}}(t) - \tilde{\theta}_3 x_{\text{fear}}(t)u_{\text{stimulus}}(t) \\ &\quad + \phi_4 x_{\text{pain}}(t)\,, &\text{(7c)}\end{aligned}$$

and

$$\begin{aligned}y_{\text{pressure}}(t) &= \tilde{\theta}_4 x_{\text{muscles}}(t) + \tilde{\theta}_5 u_{\text{pressure}}(t), &\text{(8a)}\\ y_{\text{stop}}(t) &= \phi_5 x_{\text{fear}}(t) + \tilde{\theta}_6 x_{\text{pain}}(t)\,. &\text{(8b)}\end{aligned}$$

B. Latin hypercube sampling

Since our parameters are uninterpretable, we use Latin Hypercube Sampling (LHS) to generate diverse parameter combinations and determine a reasonable range of the parameter search space.

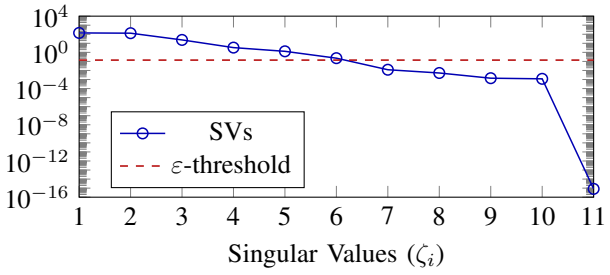

Fig. 4: Singular value spectrum for determining the rank deficiency of the COF system. We use the ε-threshold to deal with the rank deficiency and determine the number of linearly independent columns of the sensitivity matrix.

TABLE I: Parameter ranges for $\tilde{\theta}$ determined by LHS (left) and the estimated parameters and standard deviations (right).

Parameter	Lower bound	Upper bound	Initial value	Optimal value	Standard deviation
$\tilde{\theta}_1$	0.05	1	0.19	0.18	0.38
$\tilde{\theta}_2$	0.5	2	0.73	0.75	1.63
$\tilde{\theta}_3$	0	1	0.29	0.08	0.58
$\tilde{\theta}_4$	0.4	0.9	0.49	0.58	0.85
$\tilde{\theta}_5$	0.15	1	0.46	0.43	0.16
$\tilde{\theta}_6$	0	1	0.67	0.51	1.14

1) Background on Latin hypercube sampling: LHS is a statistical method that divides each variable into intervals of equal probability content [24]. LHS is designed in such a way as to create a more representative and efficient sampling of multidimensional parameter spaces; as opposed to random sampling. The general method of LHS is:

(i) Define the parameter ranges.
(ii) Divide the ranges into equal intervals.
(iii) Create a set of samples ensuring that each interval is sampled exactly once.
(iv) Ensure that the samples are evenly distributed over the parameter space.

2) Latin hypercube sampling for the COF: We use this approach to reduce the parameter space of $\tilde{\theta}$ by analyzing the best ranges for each parameter and setting a reasonable initial condition. We use 50 hypercubes within the range of $[0, 6]$, where 6 was chosen based on some initial simulations, to set initial conditions for the parameter estimation. We then set a threshold for the final cost of the parameter estimation, and order the parameter estimates based on cost. The rounded upper and lower parameter estimates within this set are then used for the bounds, see Table I.

C. Parameter estimation with online-offline measurements

We consider here the problem of identifying the parameters $\tilde{\theta}$ for (7) and (8) with the available measurement data. We begin by assuming additive, normally distributed, uncorrelated measurement errors $\varepsilon_k \sim \mathcal{N}(0, \sigma_k)$, then the measurement data is given by

$$y_M(t_k) = h(x_{\mathrm{COF}}, u, \theta^*, t_k) + \varepsilon_k \,, \tag{9}$$

where θ^* are the true parameters. Then the error of the k-th observation is given by

$$e(t_k, \theta) = y(u, \theta, t_k) - y_M(t_k) \,. \tag{10}$$

The model parameters, θ, can then be estimated by finding the parameter vector that minimizes the weighted least squares problem:

$$\hat{\theta} = \arg\min \Phi_{\mathrm{WLS}}(u, \theta) \,, \tag{11}$$

where

$$\begin{aligned} \Phi_{\mathrm{WLS}}(u, \theta) &= \sum_{i=1}^{N} w_{ii} e(t_i, \theta)^2 \\ &= (Y_M - Y(u, \theta))^\top W (Y_M - Y(u, \theta)) \,, \end{aligned}$$

and W, with diagonal elements w_{ii}, includes both the measurement uncertainty and varying weights for online vs. offline measurements, i.e., due to data sparsity, the stops are weighted differently against the pressure measurements.

We can moreover use the sensitivities from (4) to calculate predefined gradients for faster and more robust PI optimization by exploiting that

$$\frac{\mathrm{d}\Phi_{\mathrm{WLS}}(u, \theta)}{\mathrm{d}\theta} = -2 \frac{\mathrm{d}Y(u, \theta)}{\mathrm{d}\theta}^\top W (Y_M - Y(u, \theta)) \,. \tag{12}$$

V. Results

Following the methods in Section IV-C, the patient data was segmented per film and randomly allocated to an 80–20 identification-validation set. In Table II, we present the results for different modeling techniques, comparing the online-offline method against black-box models. Specifically, an ARMAX structure was selected as the best one based on an iterative exploration of various black-box models and model orders, including ARX, ARMAX, NLARX, Box-Jenkins, and output error models.

Table I displays the estimated model parameters and their corresponding standard deviations, derived from sensitivity analysis, illustrating the parameter estimation's volatility in obtaining a generalized patient model.

Table II demonstrates that the proposed grey-box model has significantly better predictive capabilities associated with pain and fear but falls short of outperforming the ARMAX model in pressure prediction. This contrast is further evident in Figures 5–7, where the models are plotted using a random patient dataset. In Figure 7, the grey-box method effectively predicts stop events, while the ARMAX model shows only a marginal increase in the predicted stop variable, see magnification. Notably, in Figure 6, the ARMAX model excels in predicting the pressure trend, but the grey-box model provides a better prediction for the peak pressure.

TABLE II: Predictive capabilities of the different models as fit values (mean $\pm$ standard deviation), i.e., $\mathrm{fit} = 100\left(1 - \frac{\|Y_M - Y\|_2}{\|Y_M - \bar{Y}_M\|_2}\right)$, where Y_M is the validation data with mean $\bar{Y}_M$, Y is the predicated value, and $\|\cdot\|_2$ is the $\mathcal{L}_2$-norm. A higher fit value indicates a better model performance.

Model	Pressure Fit	Stop Fit
ARMAX	44.68 ± 17.63	0.2691 ± 0.0575
Grey-box online-offline	28.41 ± 12.29	7.291 ± 4.689

VI. Conclusion

In this paper, we showed how one could obtain a parameterized model for predicting pain and fear as a response to pressure and erotic stimuli. We proposed a method for dealing with ill-posed systems, with parameters of low interpretability, and some offline or sparse measurements (occurring frequently in biological and medical experiments). The proposed method resulted in a parameterized model where the stop events, based on fear and pain, are predicted significantly better than classical linear time-invariant (LTI) black box models.

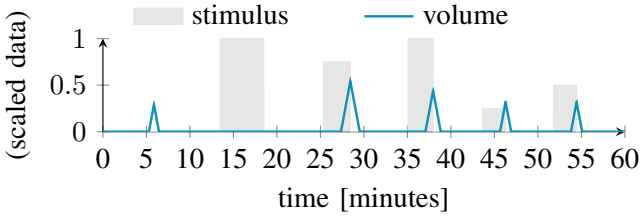

Fig. 5: Input volumes and stimulus types.

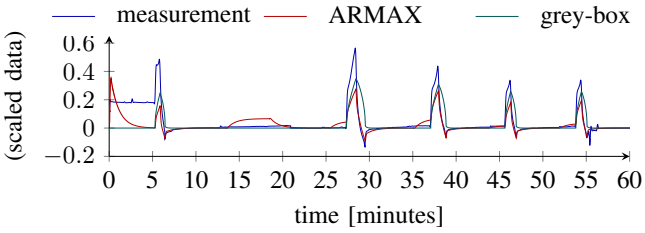

Fig. 6: Output pressure fits for different model types.

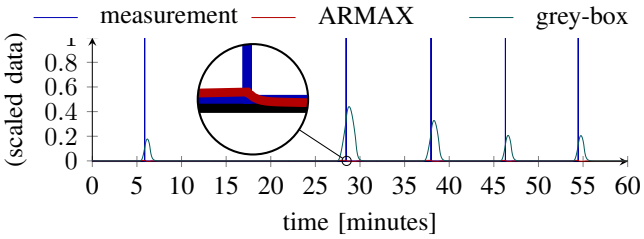

Fig. 7: Prediction of stops for different model types.

The investigated model structure was inspired by the correlations found in medical literature which were used to obtain the original qualitative model. We then aimed to validate the proposed model using medical trial data to obtain a quantitative model. The model structure, however, could be questioned based on the lack of linearity in the real data and the practical identifiability analysis indicating that only six of the eleven model parameters are identifiable. These factors indicate some limitations, that we believe may be at least partially mitigated by using different model structures or deep learning approaches for non-linear systems.

We additionally note the presence of data that is unused in our model, i.e., the subjective pleasure ratings shown in Figure 3. We propose that the subjective pleasure ratings could work as an inhibiting factor for the Circle Of Fear (COF) model or could aid in the investigation of the influence of the Circle Of Pleasure (COP) on the COF and thus provide further insight into the pain and pleasure characteristics.

Lastly, patient models are highly subject-dependent. This questions the viability of using a generalized model for predicting patient outcomes, especially for events such as stopping due to fear, where the combination of fear and pain which leads to an individual stopping the experiment would be highly subject-dependent, which questions the use of a grey-box model to improve medical treatment.

REFERENCES

[1] A. Goldstein, C. Pukall, and I. Goldstein, *Female Sexual Pain Disorders*. John Wiley & Sons, 2009.

[2] T. P. Canavan and C. D. Heckman, "Dyspareunia in women," *Postgraduate Madicine*, vol. 180, no. 2, pp. 149–166, 2000.

[3] J. A. Levy, D. C. Edwards, P. Cutruzzula-Dreher, B. H. McGreen, S. Akanda, S. Tarry, L. H. Belkoff, and K. L. Rumer, "Male-to-Female Gender Reassignment Surgery: An Institutional Analysis of Outcomes, Short-term Complications, and Risk Factors for 240 Patients Undergoing Penile-Inversion Vaginoplasty," *Urology*, 2019.

[4] K. Macey, A. Gregory, D. Nunns, and R. das Nair, "Women's experiences of using vaginal trainers (dilators) to treat vaginal penetration difficulties diagnosed as vaginismus: A qualitative interview study," *BMC Women's Health*, vol. 15, no. 1, pp. 1–12, 2015.

[5] J. van der Velde, E. Laan, and W. Everaerd, "Vaginismus, a Component of a General Defensive Reaction. An Investigation of Pelvic Floor Muscle Activity during Exposure to Emotion-Inducing Film Excerpts in Women with and without Vaginismus," *International Urogynecology Journal*, vol. 12, no. 5, pp. 328–331, 2001.

[6] S. Both, R. van Lunsen, P. Weijenborg, and E. Laan, "A New Device for Simultaneous Measurement of Pelvic Floor Muscle Activity and Vaginal Blood Flow: A Test in a Nonclinical Sample," *The Journal of Sexual Medicine*, vol. 9, no. 11, pp. 2888–2902, 2012.

[7] H. Van Lunsen and M. Ramakers, "The hyperactive pelvic floor syndrome," *Acta endoscopica*, vol. 32, no. 3, pp. 275–285, 2002.

[8] Y. M. Binik, S. Bergeron, and S. Khalifé, "Dyspareunia and vaginismus: so-called sexual pain," in *Principles and practice of sex therapy*. The Guilford Press, 2006, ch. 5, pp. 124–156.

[9] M. Brauer, E. Laan, and M. M. ter Kuile, "Sexual Arousal in Women with Superficial Dyspareunia," *Archives of Sexual Behavior*, 2006.

[10] M. A. Farmer and C. M. Meston, "Predictors of genital pain in young women." *Arch. of sexual behavior*, vol. 36, no. 6, pp. 831–43, 2007.

[11] M. M. ter Kuile, S. Both, and J. van Lankveld, "Cognitive Behavioral Therapy for Sexual Dysfunctions in Women," *Psychiatric Clinics of North America*, vol. 33, no. 3, pp. 595–610, 2010.

[12] D. Varagnolo, S. Knorn, R. Melles, and M. Dewitte, "Qualitative modeling of pressure vs. pain relations in women suffering from dyspareunia," in *IFAC World Congress*, 2017.

[13] R. Melles, M. Dewitte, M. M. ter Kuile, C. Bonnemayer, and M. Peters, "The vaginal pressure inducer: A new device to test the (un)pleasurableness and tolerance of vaginal pressure and the influence of sexual stimuli," *Journal of Sex & Marital Therapy*, 2018.

[14] L. Q. P. Paterson, R. Amsel, and Y. M. Binik, "Pleasure and pain: The effect of (almost) having an orgasm on genital and nongenital sensitivity," *Journal of Sexual Medicine*, vol. 10, no. 6, pp. 1531–1544, 2013.

[15] X. Xia and C. H. Moog, "Identifiability of nonlinear systems with application to HIV/AIDS models," *IEEE Transactions on Automatic Control*, vol. 48, no. 2, pp. 330–336, 2003.

[16] S. Audoly, G. Bellu, L. D'angiò, M. P. Saccomani, and C. Cobelli, "Global identifiability of nonlinear models of biological systems," *IEEE Transactions on Biomedical Engineering*, vol. 48, no. 1, pp. 55–65, 2001.

[17] A. F. Villaverde, "Observability and Structural Identifiability of Nonlinear Biological Systems," *Complexity*, vol. 2019, 2019.

[18] D. C. López C., T. Barz, S. Körkel, and G. Wozny, "Nonlinear ill-posed problem analysis in model-based parameter estimation and experimental design," *Computers & Chemical Engineering*, vol. 77, pp. 24–42, 2015.

[19] T. Barz, A. Sommer, T. Wilms, P. Neubauer, and M. N. Cruz Bournazou, "Adaptive optimal operation of a parallel robotic liquid handling station," *IFAC-PapersOnLine*, vol. 51, no. 2, pp. 765–770, 2018, 9th Vienna International Conference on Mathematical Modelling.

[20] P. C. Hansen, *Rank-deficient and discrete ill-posed problems: numerical aspects of linear inversion*. SIAM, 1998.

[21] D. A. Belsley, E. Kuh, and R. E. Welsch, *Regression diagnostics: Identifying influential data and sources of collinearity*. John Wiley & Sons, 2005.

[22] R. Brun, M. Kühni, H. Siegrist, W. Gujer, and P. Reichert, "Practical identifiability of asm2d parameters—systematic selection and tuning of parameter subsets," *Water research*, vol. 36, no. 16, pp. 4113–4127, 2002.

[23] R. Doshmanziari, R. R. Jackson, D. Varagnolo, and S. Knorn, "Data-driven modeling of fatigue effects following repeated muscular contractions," in *IEEE 61st CDC*, 2022, pp. 6052–6057.

[24] M. D. McKay, "Latin hypercube sampling as a tool in uncertainty analysis of computer models," in *Proceedings of the 24th conference on Winter simulation*, 1992, pp. 557–564.